# ALTERNATIVE STUDY OF A BEVEL PUNCH-ASSISTED ECAE SCHEME

*Alexander V. Perig [1)*], Nikolai N. Golodenko [2)]*
*[1)] Donbass State Engineering Academy, Manufacturing Processes and Automation Engineering Department, Kramatorsk, Ukraine*
*[2)] Donbass National Academy of Civil Engineering and Architecture, Department of Water Supply, Water Disposal and Water Resources Protection, Kramatorsk, Ukraine*

Received: 27.08.2018
Accepted: 01.10.2018

[*]*Corresponding author: e-mail: olexander.perig@gmail.com, Tel.: +380 95 169 5735, Manufacturing Processes and Automation Engineering Department, Faculty of Machine Automation and Information Technology, Donbass State Engineering Academy, Akademichna (Shkadinova) Str. 72, 84313, Kramatorsk, Ukraine*

**Abstract**
It is a common practice in pressure forming to make an Equal Channel Angular Extrusion (ECAE) of a workpiece through a die with channel intersection angle $2\theta = 90°$ using a standard punch of brick or cylindrical shape with $2\theta_0 = 90°$. However Nejadseyfi et al (2015) have applied a beveled $2\theta_0$-punch to the process of ECAE through a standard angular die of Segal geometry with $2\theta = 90°$ and $2\theta_0 \neq 2\theta$. The scope of the article is focused on an alternative numerical study of Nejadseyfi-ECAE-Scheme using techniques of Computational Fluid Dynamics (CFD). A finite-difference method was applied to the numerical solution of the boundary value problem for the Navier-Stokes equations in the form of a vorticity transfer equation. The complex of 2D plots for CFD-derived fields of flow lines and flow velocities and 3D plots for spatial distributions of flow velocities and tangential stresses were firstly derived for Nejadseyfi-ECAE-Scheme during viscous flow of polymer workpiece models through angular die with $2\theta = 90°$ for the different punch inclination angles $30° \leq 2\theta_0 \leq 150°$. It was found that Nejadseyfi-ECAE-Scheme provides enhancement of the rotary modes of intensive deformations during ECAE. Results provide visualization of velocity gradients and macroscopic rotation and the illustration of Nejadseyfi et al's ideas from an alternative CFD-based viewpoint.

**Keywords:** Equal Channel Angular Extrusion, bevel punch, inclined punch, Computational Fluid Dynamics, finite-difference method, Severe Plastic Deformation

## 1 Introduction

Equal Channel Angular Extrusion (ECAE) or Pressing (ECAP) [1-91] is a modern material processing technology, which has attracted a lot of research attention from materials science community [1-91].

The development of applications of the bevel edge (inclined) punch for ECAE dies is probably as old as the ECAE scheme itself. Today we know that the development of applications of the bevel edge punch for Equal Channel Angular Extrusion (ECAE) dies originated 30 years ago in Moscow, USSR, 1987 in restricted-access Russian-language research of such scientists as Mikhalevich V.M. [39-41, 80-81], Vaitsekhovich S.M. [80-81] et al.

DOI 10.12776/ams.v24i4.1147 p-ISSN 1335-1532
e-ISSN 1338-1156

Independently Perig et al (2015, 2017) have reported research in the ECAE application of bevel edge $2\theta_0$-punches to an angular extrusion through $2\theta$-dies ($2\theta_0 = 2\theta$, $2\theta \neq 90°$) in Perig et al's FEM-based [53], CFD-based [54, 60], and circular gridlines-based [61] articles.
Independently and simultaneously have appeared an alternative original research article by Nejadseyfi et al (2015-2016), which was focused on the application of an inclined $2\theta_0$-punch to ECAE through an angular die with channel intersection angle with $2\theta = 90°$ and punch inclination angle $2\theta_0 \neq 2\theta$ [43-44].
The purpose of the present research study is to provide an analysis of geometric and energy-power parameters of Nejadseyfi et al's ECAE scheme [43-44] from CFD-based viewpoint [42, 46, 50-51, 54, 56-58, 60, 92-98].

## 2 Materials and Methods

The theoretical method of this article used computational techniques of computational fluid dynamics (CFD) [42, 46, 50-51, 54, 56-58, 60, 92-98].
CFD-based approach of the present research was grounded on the numerical Finite-Difference Method-grounded (FDM) solution the Vorticity (Curl) Transfer Equation (V(C)TE) (1) with the boundary conditions (2):

$$\begin{cases} \dfrac{\partial \zeta}{\partial t} = -\mathbf{Re}\left( \dfrac{\partial (u\zeta)}{\partial x} + \dfrac{\partial (v\zeta)}{\partial y} \right) + \left( \dfrac{\partial^2 \zeta}{\partial x^2} + \dfrac{\partial^2 \zeta}{\partial y^2} \right); \\ \zeta = \dfrac{\partial u}{\partial y} - \dfrac{\partial v}{\partial x}; \end{cases} \tag{1.}$$

$$(\mathrm{BCs}) = \begin{pmatrix} \text{boundary } AB: & \psi_{i,30} = 1; & \zeta_{i,30} = 2\left(\psi_{i,29} - \psi_{i,30}\right)/\left(\eta^2\right); & u_{i,30} = 0; & v_{i,30} = 0; \\ \text{boundary } BC: & \psi_{50,j} = 1; & \zeta_{50,j} = 2\left(\psi_{51,j} - \psi_{50,j}\right)/\left(\xi^2\right); & u_{50,j} = 0; & v_{50,j} = 0; \\ \text{boundary } DE: & \psi_{i,0} = 0; & \zeta_{i,0} = 2\left(\psi_{i,1} - \psi_{i,0}\right)/\left(\eta^2\right); & u_{i,0} = 0; & v_{i,0} = 0; \\ \text{boundary } EF: & \psi_{80,j} = 0; & \zeta_{80,j} = 2\left(\psi_{79,j} - \psi_{80,j}\right)/\left(\xi^2\right); & u_{80,j} = 0; & v_{80,j} = 0; \\ \text{boundary } AD: & \psi_{i,j} = j/30; & \zeta_{i,j} = 0; & u_{i,j} = 1; & v_{i,j} = 0; \\ \text{pp. } A, D, E: & \psi_{i,j} = 0; & \zeta_{i,j} = 0; & & \\ \text{p. } B: & \text{for } \zeta_{51,30} \Rightarrow & \zeta_{50,30} = 2\left(\psi_{51,30} - \psi_{50,30}\right)/\left(\xi^2\right); & & \\ \text{p. } B: & \text{for } \zeta_{50,29} \Rightarrow & \zeta_{50,30} = 2\left(\psi_{50,29} - \psi_{50,30}\right)/\left(\eta^2\right); & & \\ \text{boundary } CF: & \psi_{i,80} = \psi_{i,79}; & \zeta_{i,80} = \zeta_{i,79}; & & \end{pmatrix} \tag{2.}$$

where: $\{x \,\&\, y\}$ are dimensionless coordinates (e.g. coordinates of flow lines in **Fig. 1(a)**, **Fig. 1(c)**, **Fig. 4(a)**, **Fig. 4(c)**, **Fig. 7(a)**, **Fig. 7(c)**, **Fig. 10(a)**, **Fig. 10(c)**, **Fig. 13(a)**);
$\{\xi \,\&\, \eta\}$ are the quantities of coordinate steps along axes $\{x \,\&\, y\}$;
$\{i \,\&\, j\}$ are the numbers of coordinate cells along directions $\{x \,\&\, y\}$;
$t$ is the dimensionless time of the ECAE process;
**Re** is the dimensionless Reynolds number of the flowing model of pressure worked material;
$w = \{u, v\}$ is the dimensionless full flow velocity of the flowing material **(Fig. 1(b), Fig. 1(d), Fig. 3(a), Fig. 3(c), Fig. 4(b), Fig. 4(d), Fig. 6(a), Fig. 6(c), Fig. 7(b), Fig. 7(d), Fig. 9(a), Fig. 9(c), Fig. 10(b), Fig. 10(d), Fig. 12(a), Fig. 12(c), Fig. 13(b), Fig. 15(a))**;
$u = w_x$ and $v = w_y$ are $x$– and $y$–directed dimensionless projections of the dimensionless full velocity;

DOI 10.12776/ams.v24i4.1147 p-ISSN 1335-1532
e-ISSN 1338-1156

$\zeta$ is the dimensionless vorticity (curl) function **(Fig. 2(b), Fig. 2(d), Fig. 5(b), Fig. 5(d), Fig. 8(b), Fig. 8(d), Fig. 11(b), Fig. 11(d), Fig. 14(b))**;
$\psi$ is the dimensionless stream (flow) function **(Fig. 2(a), Fig. 2(c), Fig. 5(a), Fig. 5(c), Fig. 8(a), Fig. 8(c), Fig. 11(a), Fig. 11(c), Fig. 14(a))**;
$\partial\zeta/\partial t$ is the dimensionless rate of change of the dimensionless quantity $\zeta$;
boundary conditions (2) assume an adhesion of ECAE-processed material to the internal walls of an angular die.

## 3 Results

Computational plots in **Figs. 1 – 15** have been derived by the FDM-based solution of the system (1)-(2) for the following numerical values of system parameters: the dimensional density of the worked material is $\rho^* = 1850$ kg/m$^3$; the dimensional width of the ECAE die channels (characteristic dimension) is $a^* = 40$ mm; the dimensional ECAE punching velocity is $U_0^* = 200$ mcm/s; the relative error of iterations is $e = 10^{-3}$; the dimensional time moment for building of the first isochronous contour 1 is $t_1^* = 20$ s; the dimensional time step is $t_s^* = 1.00$ mcs; the dimensional transition time is $t_{tr}^* = 80$ mcs; the dimensional time intervals between points and circles of the flow lines are 2 s and 20 s respectively; the dimensional step of time iterations is $\tau^* = 1$ μs; the dimensional coordinate step is 2 mm; the quantity of coordinate steps along the channel width is $q = 30$; the number of steps of coordinate mesh along $x$– and $y$–directions is 80 and 80, respectively; the dimensional kinematic viscosity of the pressure worked fluid model is $\upsilon^* = 0.073$ m$^2$/s; the dimensional dynamic viscosity of the fluid model is $\eta^* = 135$ Pa▪s; the dimensional yield (flow) stress of the plasticine model is $\sigma_s^* = 217$ kPa [99]; the dimensional specific heat of the plasticine model is $c^* = 1.004$ kJ/(kg▪K); the dimensional thermal conductivity of the plasticine fluid is $\lambda^* = 0.7$ J/(m▪s▪K) [100]; the dimensionless Reynolds number of the viscous plasticine model is $\mathbf{Re} = (U_0^* \text{▪} a^* \text{▪} \rho^*)/\eta^* = (U_0^* \text{▪} a^*)/\upsilon^* = 1.10 \text{▪} 10^{-4}$.

## 4 Discussion

It is important to discuss the suitability of the Newtonian fluid model (**Figs. 1 – 15**) in comparison with the more sophisticated fluid models for non-Newtonian flow. It is known that for the stresses within the Bingham fluid we have the following expression:

$$\sigma = \begin{cases} \sigma_0 + \alpha \cdot \left(\dfrac{\mathrm{d}\gamma}{\mathrm{dt}}\right), & \left(\dfrac{\mathrm{d}\gamma}{\mathrm{dt}}\right) > 0; \\ \sigma_0 - \alpha \cdot \left(\dfrac{\mathrm{d}\gamma}{\mathrm{dt}}\right), & \left(\dfrac{\mathrm{d}\gamma}{\mathrm{dt}}\right) < 0 \end{cases}$$

[92-98]. For the steady-state (stationary) flow, we have everywhere within the Bingham fluid that $\sigma > \sigma_0$ and the dependence $\sigma - \sigma_0 = \alpha \cdot \left(\dfrac{\mathrm{d}\gamma}{\mathrm{dt}}\right)$ has a linear character. Therefore, the velocity distribution within the Bingham fluid is the same as for the Newtonian fluid with $\sigma = \alpha \cdot \left(\dfrac{\mathrm{d}\gamma}{\mathrm{dt}}\right)$ (**Figs. 1 – 15**). Hence, the location of a deformation zone within the extruded Bingham fluid will be the same as for the extrusion of the Newtonian fluid with $\sigma = \alpha \cdot \left(\dfrac{\mathrm{d}\gamma}{\mathrm{dt}}\right)$ (**Figs. 1 – 15**).

DOI 10.12776/ams.v24i4.1147 p-ISSN 1335-1532
e-ISSN 1338-1156

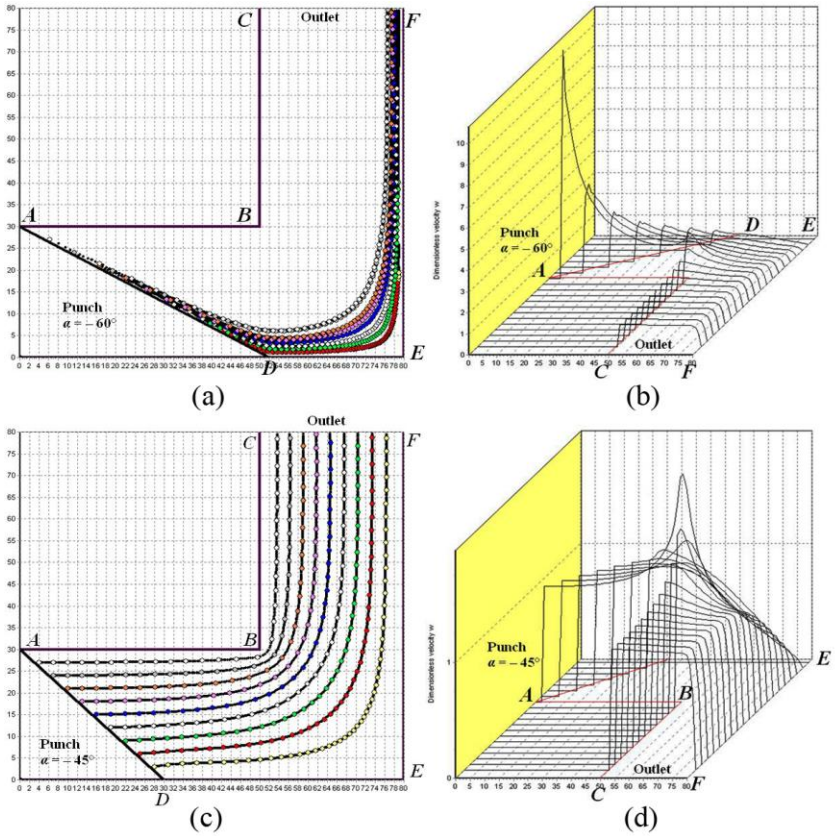


**Fig. 1** CFD-derived 2D plots of flow lines ((a), (c)) and 3D plots of the dimensionless full flow velocities w ((b), (d)) for ECAE through angular die with $2\theta = 90°$ for the different punch inclination angles $2\theta 0 = \{30°$(Fig. 1(a) – Fig. 1(b)), $45°$(Fig. 1(c) – Fig. 1(d))}, where inlet is from the left ((a) – (d)), outlet is upwards in ((a), (c)) and outlet is in our direction in ((b), (d))

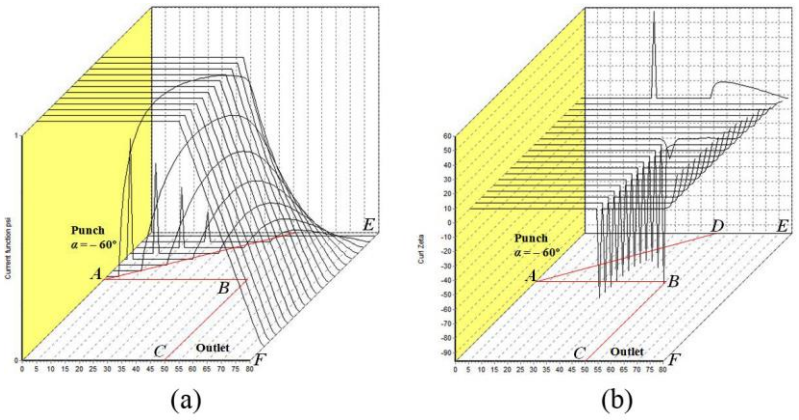


DOI 10.12776/ams.v24i4.1147 p-ISSN 1335-1532
e-ISSN 1338-1156

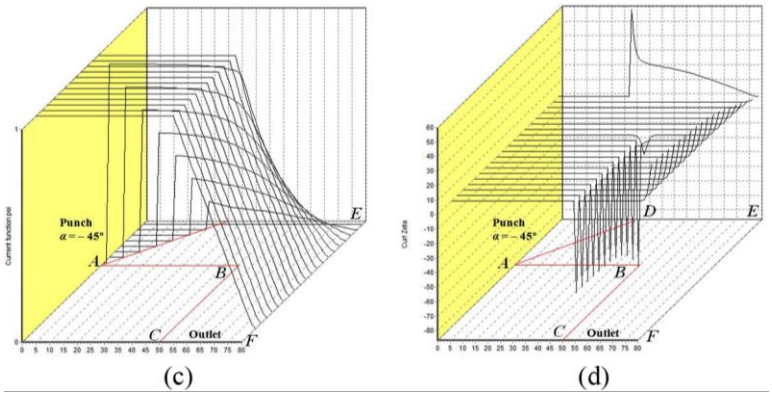


**Fig. 2** CFD-derived 3D plots of the dimensionless stream (flow) functions $\psi$ (**(a)**, **(c)**) and the dimensionless vorticity (curl) functions $\zeta$ (**(b)**, **(d)**) for ECAE through angular die with $2\theta = 90°$ for the different punch inclination angles $2\theta_0 = \{30°$(**Fig. 2(a)** – **Fig. 2(b)**), $45°$(**Fig. 2(c)** – **Fig. 2(d)**)}, where inlet is from the left in (**(a)** – **(d)**), and outlet is in our direction in (**(a)** – **(d)**)

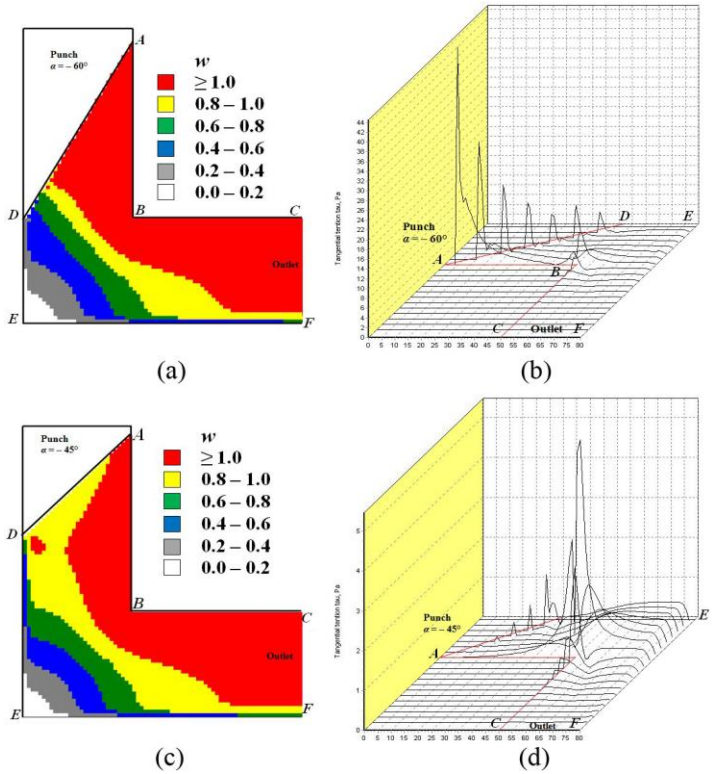


**Fig. 3** CFD-derived 2D plots of the dimensionless full flow velocities w ((a), (c)) and 3D plots of the dimensional tangential stresses $\tau$ [Pa] ((b), (d)) for ECAE through angular die with $2\theta = 90°$ for the different punch inclination angles $2\theta 0 = \{30°$(Fig. 3(a) – Fig. 3(b)), $45°$(Fig. 3(c) – Fig. 3(d))}, where inlet is from the top in ((a), (c)) and inlet is from the left in ((b), (d)), outlet is to the right in ((a), (c)) and outlet is in our direction in ((b), (d))

DOI 10.12776/ams.v24i4.1147 p-ISSN 1335-1532
e-ISSN 1338-1156

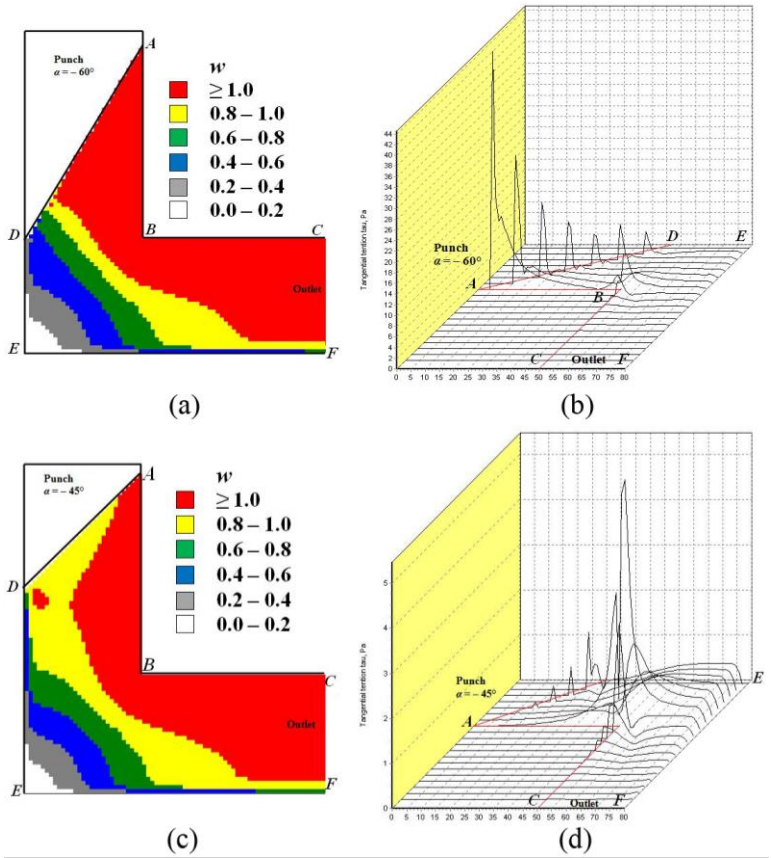


**Fig. 4** CFD-derived 2D plots of the dimensionless full flow velocities w ((a), (c)) and 3D plots of the dimensional tangential stresses τ [Pa] ((b), (d)) for ECAE through angular die with $2\theta = 90°$ for the different punch inclination angles $2\theta = \{30°$(Fig. 3(a) – Fig. 3(b)), 45°(Fig. 3(c) – Fig. 3(d))}, where inlet is from the top in ((a), (c)) and inlet is from the left in ((b), (d)), outlet is to the right in ((a), (c)) and outlet is in our direction in ((b), (d))

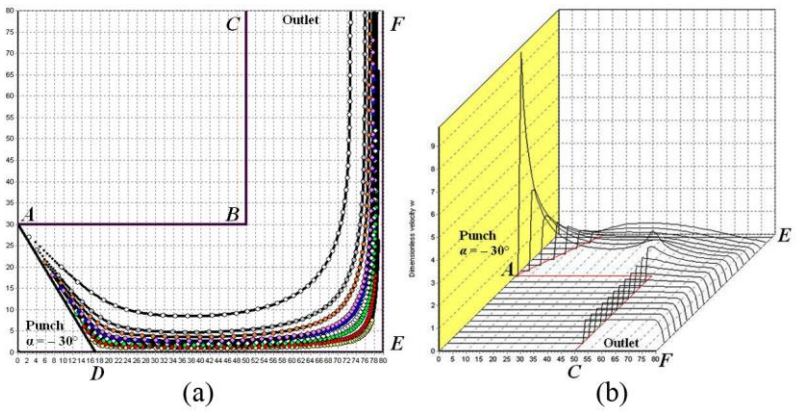


DOI 10.12776/ams.v24i4.1147 p-ISSN 1335-1532
e-ISSN 1338-1156

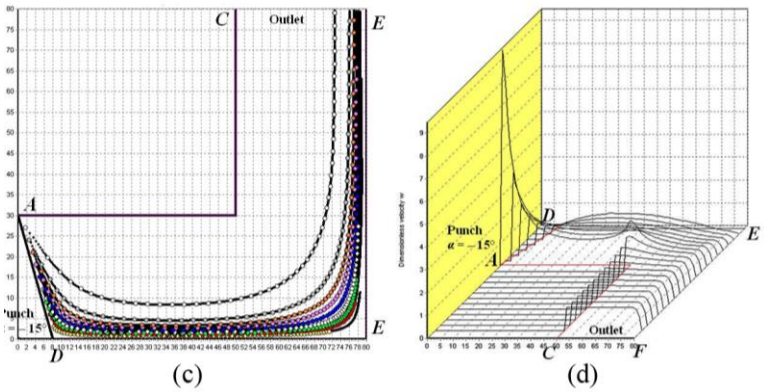


(c) (d)

**Fig. 5** CFD-derived 2D plots of flow lines ((a), (c)) and 3D plots of the dimensionless full flow velocities w ((b), (d)) for ECAE through angular die with $2\theta = 90°$ for the different punch inclination angles $2\theta 0 = \{60°$(Fig. 4(a) – Fig. 4(b)), $75°$(Fig. 4(c) – Fig. 4(d))}, where inlet is from the left ((a) – (d)), outlet is upwards in ((a), (c)) and outlet is in our direction in ((b), (d))

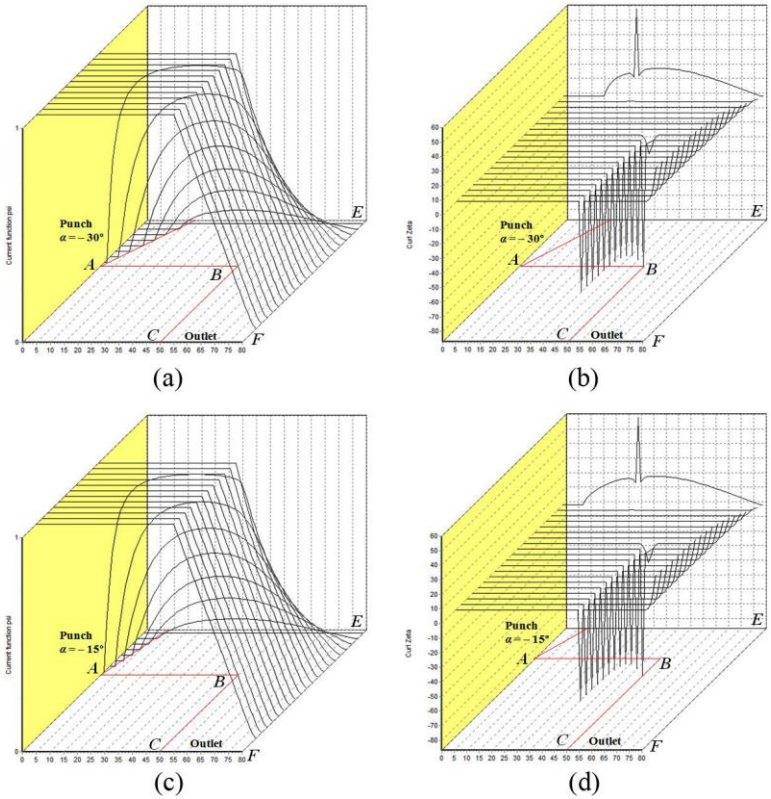


(a) (b)

(c) (d)

**Fig. 6** CFD-derived 3D plots of the dimensionless stream (flow) functions ψ ((a), (c)) and the dimensionless vorticity (curl) functions ζ ((b), (d)) for ECAE through angular die with $2\theta = 90°$ for the different punch inclination angles $2\theta 0 = \{60°$(Fig. 5(a) – Fig. 5(b)), $75°$(Fig. 5(c) – Fig. 5(d))}, where inlet is from the left in ((a) – (d)), and outlet is in our direction in ((a) – (d))

DOI 10.12776/ams.v24i4.1147 p-ISSN 1335-1532
e-ISSN 1338-1156

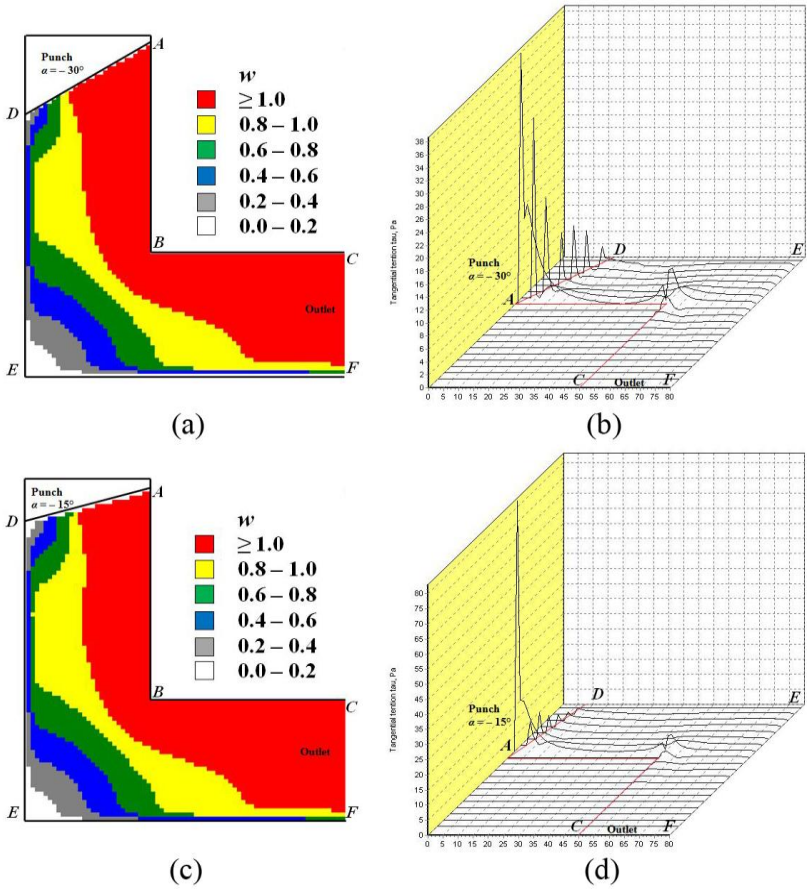


**Fig. 7** CFD-derived 2D plots of the dimensionless full flow velocities w ((a), (c)) and 3D plots of the dimensional tangential stresses τ [Pa] ((b), (d)) for ECAE through angular die with $2\theta = 90°$ for the different punch inclination angles $2\theta = \{60°$(Fig. 6(a) – Fig. 6(b)), $75°$(Fig. 6(c) – Fig. 6(d))}, where inlet is from the top in ((a), (c)) and inlet is from the left in ((b), (d)), outlet is to the right in ((a), (c)) and outlet is in our direction in ((b), (d))

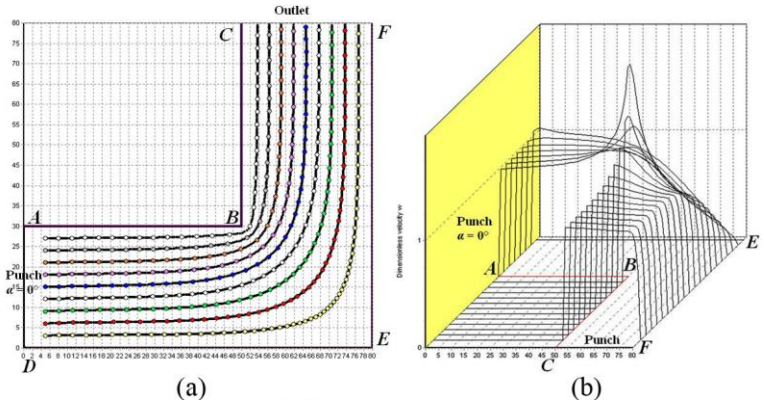


DOI 10.12776/ams.v24i4.1147 p-ISSN 1335-1532
e-ISSN 1338-1156

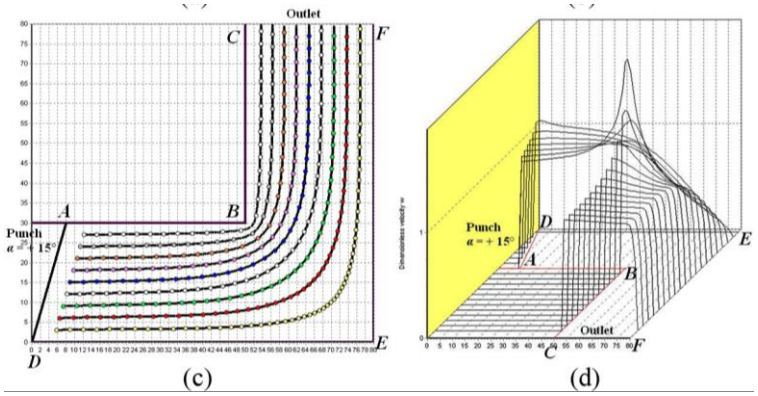


**Fig. 8** CFD-derived 2D plots of flow lines ((a), (c)) and 3D plots of the dimensionless full flow velocities w ((b), (d)) for ECAE through angular die with $2\theta = 90°$ for the different punch inclination angles $2\theta = \{90°$(Fig. 7(a) – Fig. 7(b)), $105°$(Fig. 7(c) – Fig. 7(d))}, where inlet is from the left ((a) – (d)), outlet is upwards in ((a), (c)) and outlet is in our direction in ((b), (d))

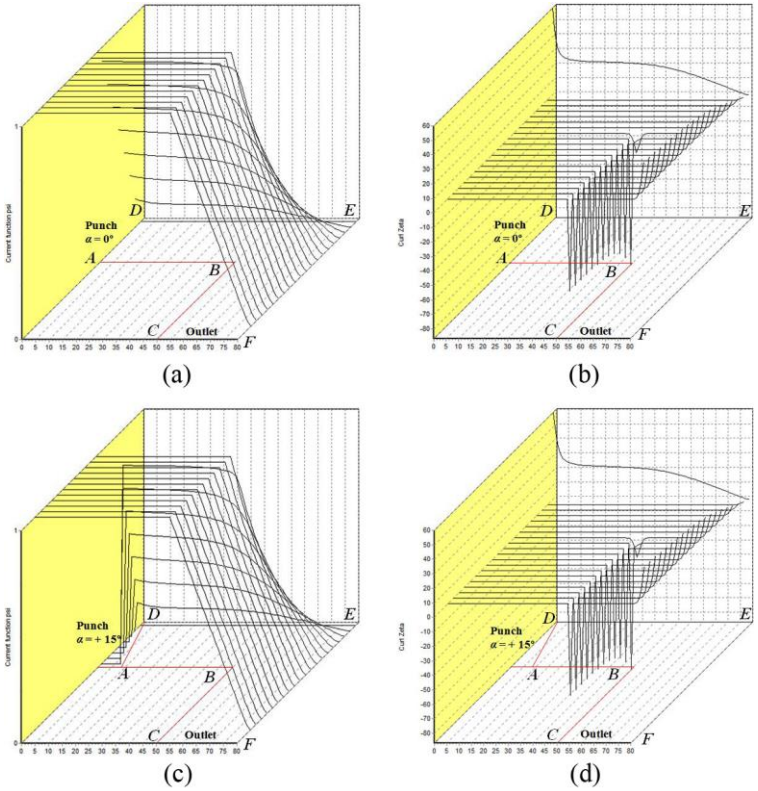


**Fig. 9** CFD-derived 3D plots of the dimensionless stream (flow) functions ψ ((a), (c)) and the dimensionless vorticity (curl) functions ζ ((b), (d)) for ECAE through angular die with $2\theta = 90°$ for the different punch inclination angles $2\theta = \{90°$(Fig. 8(a) – Fig. 8(b)), $105°$(Fig. 8(c) – Fig. 8(d))}, where inlet is from the left in ((a) – (d)), and outlet is in our direction in ((a) – (d))

DOI 10.12776/ams.v24i4.1147 p-ISSN 1335-1532
e-ISSN 1338-1156

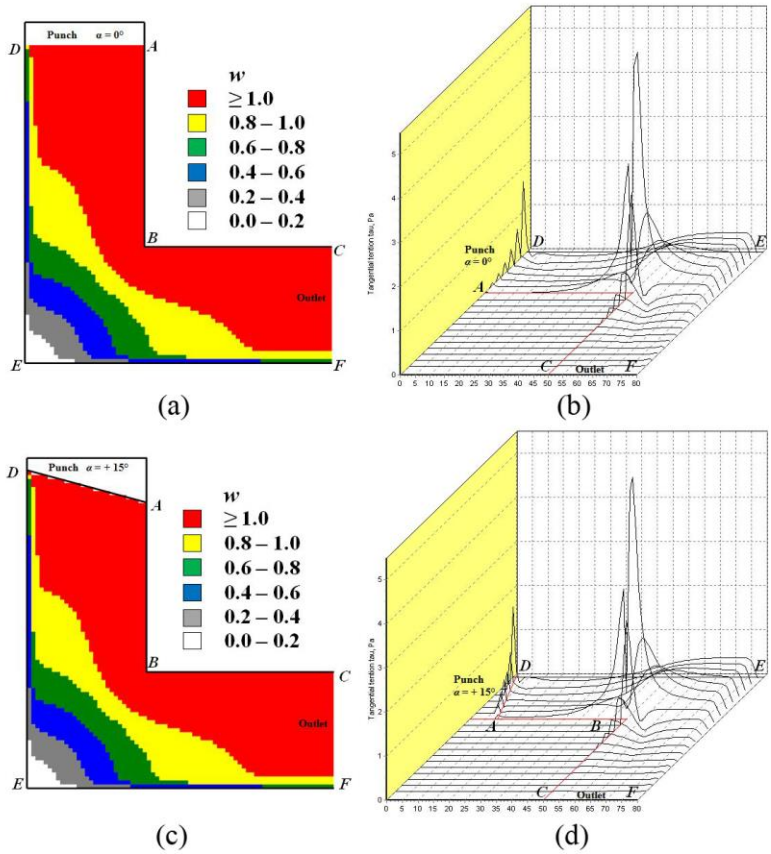


**Fig. 10** CFD-derived 2D plots of the dimensionless full flow velocities w ((a), (c)) and 3D plots of the dimensional tangential stresses τ [Pa] ((b), (d)) for ECAE through angular die with $2\theta = 90°$ for the different punch inclination angles $2\theta 0 = \{90°$(Fig. 9(a) – Fig. 9(b)), 105°(Fig. 9(c) – Fig. 9(d))}, where inlet is from the top in ((a), (c)) and inlet is from the left in ((b), (d)), outlet is to the right in ((a), (c)) and outlet is in our direction in ((b), (d))

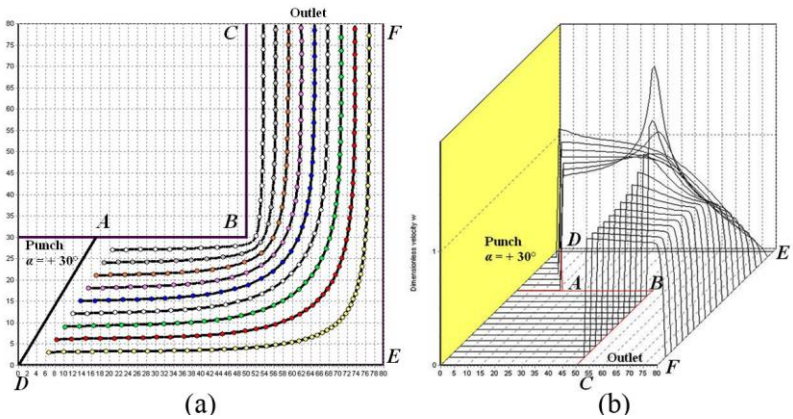


DOI 10.12776/ams.v24i4.1147 p-ISSN 1335-1532
e-ISSN 1338-1156

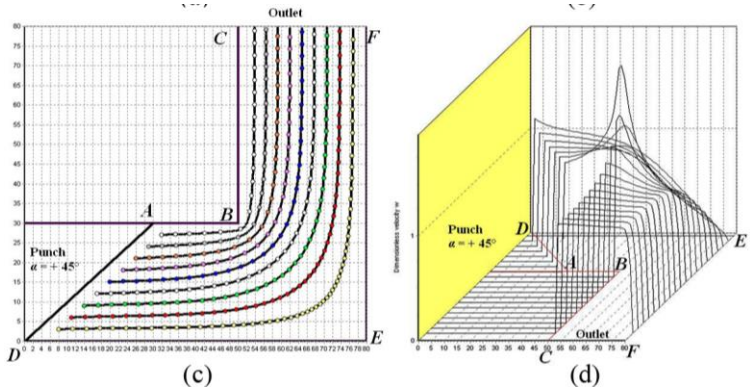


**Fig. 11** CFD-derived 2D plots of flow lines ((a), (c)) and 3D plots of the dimensionless full flow velocities w ((b), (d)) for ECAE through angular die with 2θ = 90° for the different punch inclination angles 2θ0 = {120°(Fig. 10(a) – Fig. 10(b)), 135°(Fig. 10(c) – Fig. 10(d))}, where inlet is from the left ((a) – (d)), outlet is upwards in ((a), (c)) and outlet is in our direction in ((b), (d))

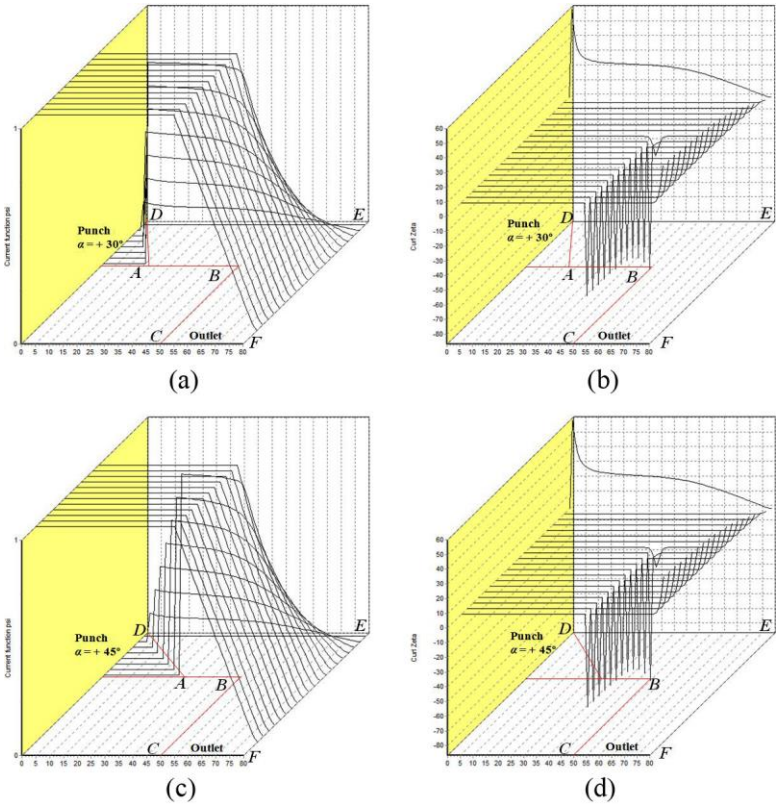


**Fig. 12** CFD-derived 3D plots of the dimensionless stream (flow) functions ψ ((a), (c)) and the dimensionless vorticity (curl) functions ζ ((b), (d)) for ECAE through angular die with 2θ = 90° for the different punch inclination angles 2θ0 = {120°(Fig. 11(a) – Fig. 11(b)), 135°(Fig. 11(c) – Fig. 11(d))}, where inlet is from the left in ((a) – (d)), and outlet is in our direction in ((a) – (d))

DOI 10.12776/ams.v24i4.1147 p-ISSN 1335-1532
e-ISSN 1338-1156

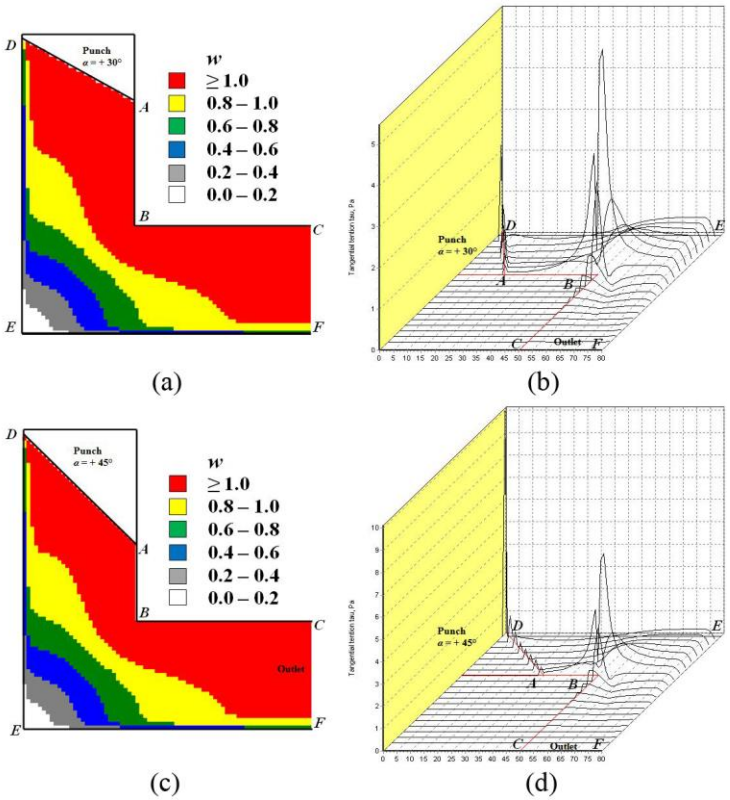


**Fig. 13** CFD-derived 2D plots of the dimensionless full flow velocities w ((a), (c)) and 3D plots of the dimensional tangential stresses τ [Pa] ((b), (d)) for ECAE through angular die with $2\theta = 90°$ for the different punch inclination angles $2\theta 0 = \{120°$(Fig. 12(a) – Fig. 12(b)), 135°(Fig. 12(c) – Fig. 12(d))}, where inlet is from the top in ((a), (c)) and inlet is from the left in ((b), (d)), outlet is to the right in ((a), (c)) and outlet is in our direction in ((b), (d))

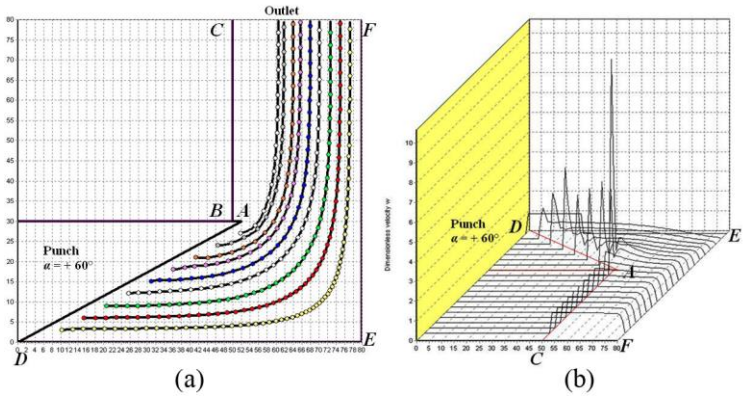


**Fig. 14** CFD-derived 2D plot of flow lines (a) and 3D plot of the dimensionless full flow velocity w (b) for ECAE through angular die with $2\theta = 90°$ for punch inclination angle $2\theta 0 = \{150°$(Fig. 13(a) – Fig. 13(b))}, where inlet is from the left ((a) – (b)), outlet is upwards in (a) and outlet is in our direction in (b)

DOI 10.12776/ams.v24i4.1147 p-ISSN 1335-1532
e-ISSN 1338-1156

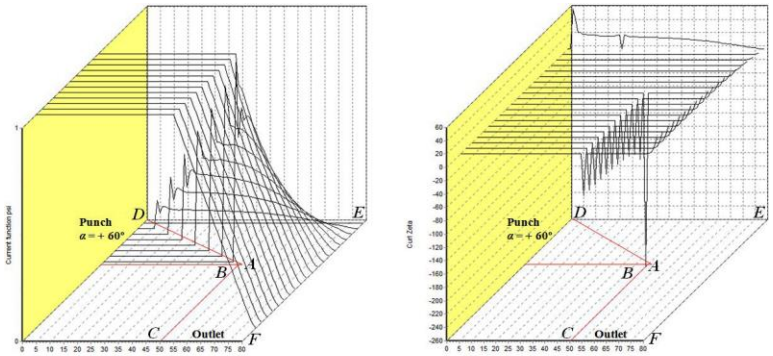


**Fig. 15** CFD-derived 3D plots of the dimensionless stream (flow) function ψ (a) and the dimensionless vorticity (curl) function ζ (b) for ECAE through angular die with 2θ = 90° for punch inclination angle 2θ0 = {150°(Fig. 14(a) – Fig. 14(b))}, where inlet is from the left in ((a) – (b)), and outlet is in our direction in ((a) – (b))

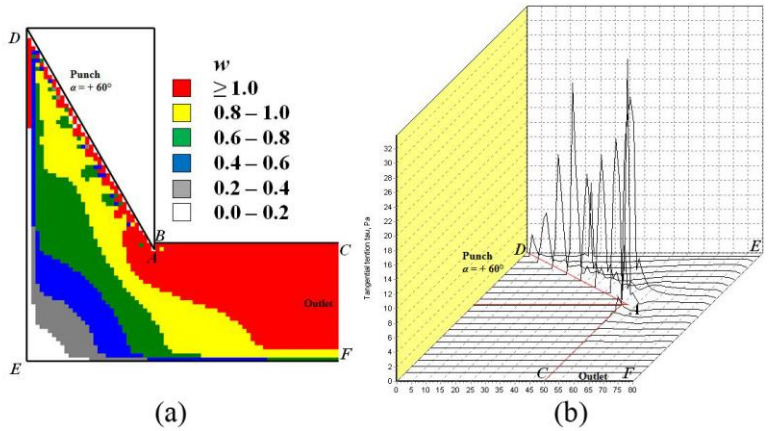


**Fig. 16** CFD-derived 2D plot of the dimensionless full flow velocities w (a) and 3D plot of the dimensional tangential stress τ [Pa] (b) for ECAE through angular die with 2θ = 90° for punch inclination angle 2θ0 = {150°(Fig. 15(a) – Fig. 15(b))}, where inlet is from the top in (a) and inlet is from the left in (b), outlet is to the right in (a) and outlet is in our direction in (b)

It is known that for a power law fluid we have $\sigma = \alpha \cdot \left( \frac{\mathrm{d}\gamma}{\mathrm{dt}} \right)^n$ [92-98]. There is no dead zone formation in a perfectly motionless (standing) area in a local flow during angular extrusion with both power law and Newtonian fluid for $\sigma < \sigma_0$ (in contrast to the Bingham fluid).

## 5 Conclusion

This present article reports a CFD-based [42, 46, 50-51, 54, 56-58, 60, 92-98] analysis of the Nejadseyfi et al's ECAE scheme [43-44].

DOI 10.12776/ams.v24i4.1147 p-ISSN 1335-1532
e-ISSN 1338-1156

The authors of the present study have formulated, derived and visualized in **Figs. 1 – 15** a CFD-grounded numerical solution of the unique Nejadseyfi et al's ECAE scheme [43-44].

The Newtonian fluid model is the first rheological approach to material flow through the angular domains in **Figs. 1 – 15**. Existence of this first rheological approach of the Nejadseyfi et al's ECAE scheme [43-44] in the present paper (**Figs. 1 – 15**) is quite possible and does not contradict the fundamental concepts of the well-known guides [92-98].

Computational CFD-based plots in **Figs. 1 – 6** show the geometric possibility of partial or complete elimination of the dead zone using acute-angled punches with punch inclination angles of $2\theta_0 = \{30°, 45°, 60°, 75°\}$.

Numerical plots in **Figs. 7 – 15** show that using obtuse-angled punches with punch inclination angles $2\theta_0 = \{105°, 120°, 135°, 150°\}$ results in the formation of successively growing areas of dead zones due to partial or complete closing of the outlet die channel with the obtuse-angled punch.

The authors of the present theoretical study using CFD-based language have shown that the original Nejadseyfi et al's investigation [43-44] reports non-standard, non-obvious and highly creative technical scheme of ECAE, which should attract more scientific attention from the growing materials science sphere of SPD-related research.

Additional analysis of Nejadseyfi et al's ECAE scheme [43-44] should be done using CFD, taking into account additional independent translational motions of the die walls and different values of die channel intersection angles in the range of $30° \leq 2\theta \leq 150°$. Completion of this study will be a matter of further research efforts by the authors.

**References**

[1] A. Abedian, B. Shirani Bidabadi, R. Shateri: International Journal on Interactive Design and Manufacturing, Vol. 12, 2018, No. 1, p. 49-61, DOI: 10.1007/s12008-017-0374-3

[2] P. Abhari: Mechanics and Advanced Technologies, Vol. 80, 2017, No. 2, p. 71-77, DOI: 10.20535/2521-1943.2017.80.109198

[3] I. Aliev, Y. Zhbankov, S. Martynov: Journal of Chemical Technology and Metallurgy, Vol. 51, 2016, No. 4, p. 393-400

[4] A. Aminnudin, P. Pratikto, A. Purnowidodo, Y. S. Irawan: Eastern-European Journal of Enterprise Technologies, Vol. 2, 2018, No. 1 (92), p. 57-62, DOI:10.15587/1729-4061.2018.127006

[5] B. Aour, F. Zaïri, R. Boulahia, M. Naït-Abdelaziz, J. M. Gloaguen, J. M. Lefebvre: Computational Materials Science, Vol. 45, 2009, No. 3, p. 646-652. DOI: 10.1016/j.commatsci.2008.08.020

[6] R. Arruffat-Massion, L. S. Tóth, J.-P. Mathieu: Scripta Materialia, Vol. 54, 2006, No. 9, p. 1667-1672, DOI: 10.1016/j.scriptamat.2006.01.004

[7] E. Bagherpour, M. Reihanianorcid, N. Pardis, R. Ebrahimiorcid, T. G. Langdon: Iranian Journal of Materials Forming, Vol. 5, 2018, No. 1, p. 71-113, DOI: 10.22099/ijmf.2018.28756.1101

[8] G. A. Baglyuk, A. P. Maidanyuk, M. B. Shtern: Powder Metallurgy and Metal Ceramics, Vol. 51, 2013, No. 9-10, p. 503–508, DOI: 10.1007/s11106-013-9461-6

[9] V. A. Beloshenko, Yu. V. Voznyak, I. Yu. Reshidova, M. Naït-Abdelaziz, F. Zairi: Journal of Polymer Research, Vol. 20, 2013, No. 12, Article number 322, p. 1-13, DOI: 10.1007/s10965-013-0322-2

[10] V. A. Beloshenko, A. V. Voznyak, Yu. V. Voznyak, L. A. Novokshonova, V. G. Grinyov, V. G. Krasheninnikov: International Journal of Polymer Science, Vol. 2016, 2016, Article number 8564245, p. 1-8, DOI: 10.1155/2016/8564245
[11] I. J. Beyerlein, C. N. Tomé: Materials Science and Engineering: A, Vol. 380, 2004, No. 1-2, p. 171-190, DOI: 10.1016/j.msea.2004.03.063
[12] Y. Beygelzimer, R. Kulagin, L. S. Toth, Y. Ivanisenko: Beilstein Journal of Nanotechnology, Vol. 7, 2016, p. 1267-1277, DOI:10.3762/bjnano.7.117
[13] Y. Beygelzimer et al.: Advanced Engineering Materials, Vol. 19, 2017, No. 8, Article number 1600873, p. 1-24, DOI: 10.1002/adem.201600873
[14] J. Bidulská et al.: Acta Physica Polonica A, Vol. 117, 2010, No. 5, p. 864-868, DOI: 10.12693/APhysPolA.117.864
[15] K. BongKi et al.: Journal of the Korean Society of Manufacturing Technology Engineers, Vol. 27, 2018, No. 1, p. 46-56, DOI: 10.7735/ksmte.2018.27.1.46
[16] R. Boulahia, J. M. Gloaguen, F. Zaïri, M. Naït-Abdelaziz, R. Seguela, T. Boukharouba, J. M. Lefebvre: Polymer, Vol. 50, 2009, No. 23, p. 5508-5517, DOI: 10.1016/j.polymer.2009.09.050
[17] T. S. Creasy, Y. S. Kang: Journal of Thermoplastic Composite Materials, Vol. 17, 2004, No. 3, p. 205-227, DOI: 10.1177/0892705704035403
[18] R. Comaneci, L. G. Bujoreanu, C. Baciu, A. M. Predescu, D. Savastru: Optoelectronics and Advanced Materials – Rapid Communications, Vol. 9, 2015, No. 9-10, p. 1322-1327
[19] R. I. Comăneci, D. Nedelcu, L. G. Bujoreanu: AIP Conference Proceedings, Vol. 1896, 2017, Article number 200004, p. 1-6, DOI: 10.1063/1.5008241
[20] Y. Estrin, A. Vinogradov: Acta Materialia, Vol. 61, 2013, No. 3, p. 782-817, DOI: 10.1016/j.actamat.2012.10.038
[21] F. Fereshteh-Saniee, A. Sepahi-Boroujeni, S. Sepahi-Boroujeni: International Journal of Advanced Manufacturing Technology, Vol. 86, 2016, No. 9-12, p. 3471-3482. DOI: 10.1007/s00170-016-8487-6
[22] W. Z. Han, Z. F. Zhang, S. D. Wu, S. X. Li: Materials Science and Engineering: A, Vol. 476, 2008, No. 1-2, p. 224-229, DOI: 10.1016/j.msea.2007.04.114
[23] A. Hasani, R. Lapovok, L. S. Tóth, A. Molinari: Scripta Materialia, Vol. 58, 2008, No. 9, p. 771-774, DOI: 10.1016/j.scriptamat.2007.12.018
[24] M. Hawryluk, J. Ziemba: Measurement: Journal of the International Measurement Confederation, Vol. 128, 2018, p. 204-213, DOI: 10.1016/j.measurement.2018.06.037
[25] M. Honarpisheh, M. Dehghani, S. Ghaffari: Journal of Modern Processes in Manufacturing and Production, Vol. 3, 2014, No. 4, p. 83-92
[26] E. Hosseini, M. Kazeminezhad: Computational Materials Science, Vol. 44, 2009, No. 4, p. 1107-1115, DOI: 10.1016/j.commatsci.2008.07.024
[27] J. Kaur, B. S. Pabla, S. S. Dhami: International Journal of Engineering Research & Technology, Vol. 5, 2016, No. 1, p. 383-393, DOI: 10.17577/IJERTV5IS010310
[28] R. Kočiško, T. Kvačkaj, J. Bidulská, M. Molnárová: Acta Metallurgica Slovaca, Vol. 15, 2009, No. 4, p. 228-233
[29] B. V. Koutcheryaev: Modeling of Continual Flows in Angular Domains. In.: *Investigations and Applications of Severe Plastic Deformation. NATO Science Series* (*Series 3. High Technology*), edited by T. C. Lowe, R. Z. Valiev, Springer, Dordrecht, Vol. 80, 2000, p. 37-42, DOI: 10.1007/978-94-011-4062-1_5

[30] B. V. Kucheryaev: *Continuum Mechanics (Theoretical Principles of the Pressure Treatment of Composite Metals with Problems and Solutions, Examples and Exercises)* [*Mekhanika sploshnykh sred (teoreticheskie osnovy obrabotki davleniem kompozitnykh metallov s zadachami i resheniiami, primerami i uprazhneniiami)*], second ed., MISiS, Moscow, 2006, (in Russian).
[31] P. Kumar, S. S. Panda: International Journal of Advanced Manufacturing Technology, Vol. 91, 2017, No. 1-4, p. 835-846, DOI: 10.1007/s00170-016-9768-9
[32] A. M. Laptev, A. V. Perig, O. Yu. Vyal: Materials Research – Ibero-american Journal of Materials, Vol. 17, 2014, No. 2, p. 359-366, DOI: 10.1590/S1516-14392013005000187
[33] Ł. Łach, J. Nowak, D. Svyetlichnyy: Journal of Materials Processing Technology, Vol. 255, 2018, p. 488-499, DOI: 10.1016/j.jmatprotec.2017.12.001
[34] S. N. Lezhnev, I. E. Volokitina, D. V. Kuis: Physics of Metals and Metallography, Vol. 119, 2018, No. 8, p. 810-815, DOI: 10.1134/S0031918X18040129
[35] H. Li, X. Huang, C. Huang, Y. Zhao: Journal of Applied Polymer Science, Vol. 123, 2012, No. 4, p. 2222-2227, DOI: 10.1002/app.34739
[36] C. J. Luis Pérez: Modelling and Simulation in Materials Science and Engineering, Vol. 12, 2004, No. 2, p. 205-214, DOI: 10.1088/0965-0393/12/2/002
[37] C. J. Luis Pérez, R. Luri: Mechanics of Materials, Vol. 40, 2008, No. 8, p. 617-628, DOI: 10.1016/j.mechmat.2008.02.003
[38] N. Medeiros, L. P. Moreira, J. D. Bressan, J. F. C. Lins, J. P. Gouvêa: Materials Science and Engineering: A, Vol. 527, 2010, No. 12, p. 2831-2844, DOI: 10.1016/j.msea.2009.12.049
[39] V. M. Mikhalevich: Strength of Materials, Vol. 27, 1995, No. 8, p. 482-492, DOI: 10.1007/BF02209347
[40] V. M. Mikhalevich: Strength of Materials, Vol. 27, 1995, No. 9, p. 549-558, DOI: 10.1007/BF02208573
[41] V. M. Mikhalevich: Strength of Materials, Vol. 28, 1996, No. 3, p. 238-246, DOI: 10.1007/BF02133202
[42] P. Minakowski: Technische Mechanik, Vol. 34, 2014, No. 3-4, p. 213-221, DOI: 10.24352/UB.OVGU-2017-063
[43] O. Nejadseyfi, A. Shokuhfar, A. Azimi, M. Shamsborhan: Journal of Materials Science, Vol. 50, 2015, No. 3, p. 1513-1522, DOI: 10.1007/s10853-014-8712-3
[44] O. Nejadseyfi, A. Shokuhfar, S. Sadeghi: Materials Science and Engineering: A, Vol. 651, 2016, p. 461-466, DOI: 10.1016/j.msea.2015.08.050
[45] D. V. Pavlenko: Powder Metallurgy and Metal Ceramics, Vol. 56, 2017, No. 5-6, p. 273-282, DOI: 10.1007/s11106-017-9895-3
[46] A. V. Perig, A. M. Laptev, N. N. Golodenko, Yu. A. Erfort, E. A. Bondarenko: Materials Science and Engineering: A, Vol. 527, 2010, No. 16-17, p. 3769-3776, DOI: 10.1016/j.msea.2010.03.043
[47] A. V. Perig, I. G. Zhbankov, V. A. Palamarchuk: Materials and Manufacturing Processes, Vol. 28, 2013, No. 8, p. 910-915, DOI: 10.1080/10426914.2013.792420
[48] A. V. Perig, I. G. Zhbankov, I. A. Matveyev, V. A. Palamarchuk: Materials and Manufacturing Processes, Vol. 28, 2013, No. 8, p. 916-922, DOI: 10.1080/10426914.2013.792417
[49] A. V. Perig, A. M. Laptev: Journal of the Brazilian Society of Mechanical Sciences and Engineering, Vol. 36, 2014, No. 3, p. 469-476, DOI: 10.1007/s40430-013-0121-z

[50] A. V. Perig, N. N. Golodenko: Chemical Engineering Communications, Vol. 201, 2014, No. 9, p. 1221-1239, DOI: 10.1080/00986445.2014.894509
[51] A. V. Perig, N. N. Golodenko: International Journal of Advanced Manufacturing Technology, Vol. 74, 2014, No. 5-8, p. 943-962, DOI: 10.1007/s00170-014-5827-2
[52] A. V. Perig: Materials Research – Ibero-american Journal of Materials, Vol. 17, 2014, No. 5, p. 1226-1237, DOI: 10.1590/1516-1439.268114
[53] A. V. Perig, A. F. Tarasov, I. G. Zhbankov, S. N. Romanko: Materials and Manufacturing Processes, Vol. 30, 2015, No. 2, p. 222-231, DOI: 10.1080/10426914.2013.832299
[54] A. V. Perig, N. N. Golodenko: Mechanical Sciences, Vol. 6, 2015, No. 1, p. 41-49, DOI: 10.5194/ms-6-41-2015
[55] A. Perig: Materials Research – Ibero-american Journal of Materials, Vol. 18, 2015, No. 3, p. 628-638, DOI: 10.1590/1516-1439.004215
[56] A. V. Perig, N. N. Golodenko: Materials Research – Ibero-american Journal of Materials, Vol. 19, 2016, No. 3, p. 602-610, DOI: 10.1590/1980-5373-MR-2016-0013
[57] A. V. Perig, N. N. Golodenko: Materials Research Express, Vol. 3, 2016, No. 11, Article number 115301, p. 1-10, DOI: 10.1088/2053-1591/3/11/115301
[58] A. V. Perig, N. N. Golodenko: Advances in Materials Science and Engineering, Vol. 2017, 2017, Article number 7015282, p. 1-26, DOI: 10.1155/2017/7015282
[59] A. V. Perig, I. S. Galan, Letters on Materials, Vol. 7, 2017, No. 3, p. 209-217, DOI: 10.22226/2410-3535-2017-3-209-217
[60] A. V. Perig, N. N. Golodenko: AIMS Materials Science, Vol. 4, 2017, No. 6, p. 1240-1275, DOI: 10.3934/matersci.2017.6.1240
[61] A. V. Perig: Journal of Materials Education, Vol. 39, 2017, No. 5-6, p. 193-208
[62] O. V. Prokof'eva, Y. Y. Beygelzimer, R. Y. Kulagin, Y. Z. Estrin, V. N. Varyukhin: Russian Metallurgy (Metally), Vol. 2017, 2017, No. 3, p. 226-230, DOI: 10.1134/S0036029517030090
[63] J. Qiu, T. Murata, X. Wu, M. Kitagawa, M. Kudo: Journal of Materials Processing Technology, Vol. 212, 2012, No. 7, p. 1528-1536, DOI: 10.1016/j.jmatprotec.2012.02.015
[64] G. J. Raab, R. Z. Valiev, T. C. Lowe, Y. T. Zhu: Materials Science and Engineering: A, Vol. 382, 2004, No. 1-2, p. 30-34, DOI: 10.1016/j.msea.2004.04.021
[65] G. I. Raab, E. I. Fakhretdinova, R. Z. Valiev, L. P. Trifonenkov, V. F. Frolov: Metallurgist, Vol. 59, 2016, No. 11-12, p. 1007-1014, DOI: 10.1007/s11015-016-0207-9
[66] N. M. Rusin: Russian Journal of Non-Ferrous Metals, Vol. 50, 2009, No. 5, p. 529-533, DOI: 10.3103/S1067821209050186
[67] D. V. Rutskii, N. A. Zyuban, S. B. Gamanyuk: CIS Iron and Steel Review, Vol. 12, 2016, p. 22-25, DOI: 10.17580/cisisr.2016.02.05
[68] D. Salcedo et al.: Materials and Manufacturing Processes, Vol. 29, 2014, No. 4, p. 434-441, DOI: 10.1080/10426914.2013.864396
[69] V. M. Segal: Materials Science and Engineering: A, Vol. 271, 1999, No. 1-2, p. 322-333, DOI: 10.1016/S0921-5093(99)00248-8
[70] V. M. Segal: Materials Science and Engineering: A, Vol. 345, 2003, No. 1-2, p. 36-46, DOI: 10.1016/S0921-5093(02)00258-7
[71] V. M. Segal: Materials Science and Engineering: A, Vol. 476, 2008, No. 1-2, p. 178-185, DOI: 10.1016/j.msea.2007.04.092
[72] V. Segal: Materials, Vol. 11, 2018, No. 7, Article number 1175, p. 1-29, DOI: 10.3390/ma11071175

[73] Y. R. Seo, J.-I. Weon: Journal of the Korean Physical Society, Vol. 63, 2013, No. 1, p. 114-119, DOI: 10.3938/jkps.63.114
[74] F. R. F. Silva, N. Medeiros, L. P. Moreira, J. F. C. Lins, J. P. Gouvêa: Materials Science and Engineering: A, Vol. 546, 2012, p. 180-188, DOI: 10.1016/j.msea.2012.03.049
[75] R. Sivak: Eastern-European Journal of Enterprise Technologies, Vol. 6, 2017, No. 7 (90), p. 34-41, DOI: 10.15587/1729-4061.2017.115040
[76] D. S. Svyetlichnyy, K. Muszka, J. Majta: Computational Materials Science, Vol. 102, 2015, Article number 6397, p. 159-166, DOI: 10.1016/j.commatsci.2015.02.034
[77] D. Svyetlichnyy, J. Nowak, N. Biba, Ł. Łach: International Journal of Advanced Manufacturing Technology, Vol. 87, 2016, No. 1-4, p. 543-552, DOI: 10.1007/s00170-016-8506-7
[78] H.-J. Sue, H. Dilan, C. K.-Y. Li: Polymer Engineering and Science, Vol. 39, 1999, No. 12, p. 2505-2515, DOI: 10.1002/pen.11638
[79] L. S. Tóth, R. A. Massion, L. Germain, S. C. Baik, S. Suwas: Acta Materialia, Vol. 52, 2004, No. 7, p. 1885-1898, DOI: 10.1016/j.actamat.2003.12.027
[80] S. M. Vaitsekhovich, V. M. Mikhalevich, V. A. Kraevskii: Powder Metallurgy and Metal Ceramics, Vol. 52, 2013, No. 1-2, p. 1-6, DOI: 10.1007/s11106-013-9489-7
[81] S. M. Vaitsekhovich, V. M. Mikhalevich, V. A. Kraevskii: Powder Metallurgy and Metal Ceramics, Vol. 52, 2013, No. 3-4, p. 132-136, DOI: 10.1007/s11106-013-9505-y
[82] A. Vinogradov, Y. Estrin: Progress in Materials Science, Vol. 95, 2018, p. 172-242, DOI: 10.1016/j.pmatsci.2018.02.001
[83] Y. Voznyak: Macromolecular Research, Vol. 25, 2017, No. 1, p. 38-44, DOI: 10.1007/s13233-017-5001-4
[84] V. Q. Vu, Y. Beygelzimer, R. Kulagin, L. S. Toth: Advances in Materials Science and Engineering, Vol. 2018, 2018, Article number 8747960, p. 1-8, DOI: 10.1155/2018/8747960
[85] K. Wei, P. Liu, Z. Ma, W. Wei, I. V. Alexandrov, J. Hu: Acta Metallurgica Slovaca, Vol. 21, 2015, No. 1, p. 4-12, DOI: 10.12776/ams.v21i1.539
[86] J. I. Weon, T. S. Creasy, H.-J. Sue, A. J. Hsieh: Polymer Engineering and Science, Vol. 45, 2005, No. 3, p. 314-324, DOI: 10.1002/pen.20269
[87] Y. Wu, I. Baker: Scripta Materialia, Vol. 37, 1997, No. 4, p. 437-442, DOI: 10.1016/S1359-6462(97)00132-2
[88] Z.-Y. Xia, H.-J. Sue, T. P. Rieker, Macromolecules, Vol. 33, 2000, No. 23, p. 8746-8755, DOI: 10.1021/ma001140w
[89] C. Xu, S. Schroeder, P. B. Berbon, T. G. Langdon: Acta Materialia, Vol. 58, 2010, No. 4, p. 1379-1386, DOI: 10.1016/j.actamat.2009.10.044
[90] A. Zavdoveev et al.: Emerging Materials Research, Vol. 4, 2015, No. 1, p. 89-93, DOI: 10.1680/emr.14.00016
[91] X. Zhang, D. Gao, X. Wu, K. Xia: European Polymer Journal, Vol. 44, 2008, No. 3, p. 780-792, DOI: 10.1016/j.eurpolymj.2007.12.011
[92] J. W. Goodwin, R. W. Hughes: *Rheology for Chemists: An Introduction*, second ed., Royal Society of Chemistry (RSC), Cambridge, UK, 2008, p. 1-58, DOI: 10.1039/9781847558046
[93] P. Oswald: *Rheophysics. The Deformation and Flow of Matter*, first ed., Cambridge University Press, New York, 2009
[94] R. L. Panton: *Incompressible flow*, third ed., John Wiley & Sons, Hoboken, USA, 2005

[95] R. A. Pethrick: *Polymer Structure Characterization: From Nano to Macro Organization*, first ed., Royal Society of Chemistry (RSC), Cambridge, UK, 2007, DOI: 10.1039/9781847557896
[96] P. J. Roache: *Fundamentals of Computational Fluid Dynamics*, first ed., Hermosa Publishers, Socorro, U.S.A., 1998
[97] M. Rubinstein, R. H. Colby: *Polymer Physics*, first ed., Oxford University Press, New York, 2003
[98] G. Strobl: *The Physics of Polymers. Concepts for Understanding Their Structures and Behavior*, third ed., Springer, Berlin, 2007, DOI: 10.1007/978-3-540-68411-4
[99] H. Sofuoglu, J. Rasty: Tribology International, Vol. 33, 2000, No. 8, p. 523-529, DOI: 10.1016/S0301-679X(00)00092-X
[100] K. Chijiiwa, Y. Hatamura, N. Hasegawa: Transactions of the Iron and Steel Institute of Japan, Vol. 21, 1981, No. 3, p. 178-186, DOI: 10.2355/isijinternational1966.21.178